Effect of steel counterface on the dry sliding behaviour of a Cu-based metal matrix composite

Priyadarshini Jayashree,[1] Matteo Federici,[1] Luca Bresciani,[2] Simone Turani,[2] Roberto Sicigliano,[2] Giovanni Straffelini[1]

[1] Department of Industrial Engineering, University of Trento, via Sommarive 9, Trento - Italy
[2] Brembo S.p.A.,

Abstract
Pin-on-disc testing was used to investigate the friction and wear behaviour of a Cu-based metal matrix composite dry sliding against three different martensitic steels. The tests were carried out at two contact pressures (0.5 and 1 MPa) and two sliding velocities (1.57 and 7 m/s), and the results were explained by considering the characteristics of the friction layers formed on the pin and disc surfaces during sliding. At 7 m/s, pin and disc wear was very mild in every condition, because the high flash temperatures achieved during sliding induced intense oxidation of the disc asperities, irrespective of the steel disc compositions. At 1.57 m/s, the steel composition played an important role. When using a heat-treated steel and a conventional martensitic stainless steel, pin and disc wear was by 'low-sliding speed tribo-oxidation', regarded as mild wear. However, when using a martensitic stainless steel with a very high Cr-content and a very low C-content, i.e., by a very high oxidation resistance, pin and disc wear was by adhesion/delamination at 0.5 MPa, and thus severe in nature. The results presented herewith clearly suggest the importance of selecting suitable steel counterfaces in the optimization of the tribological systems tribological involving Cu-based metal matrix composites as a mating material.

Keywords Sliding wear, Cu-based metal matrix composite, Friction layer, Tribo-oxidative wear.

1 Introduction

Copper-based metal matrix composites are employed under dry sliding condition against a steel counterface in different applications. In fact, copper and iron display a relatively low tribological compatibility, their alloys can be hardened to bear the contact stress better, and the high thermal conductivity of copper alloys allows maintaining low contact temperatures during sliding with beneficial effects on the system wear behaviour [1, 2]. All these aspects are regarded as very attractive tribological properties.

An important example of these materials is constituted by Cu-based composites produced by powder metallurgy (PM), and used in brake pads for train or aircraft applications [3-6]. In addition to a pure Cu or a Cu alloy matrix, these materials typically contain: graphite, that is a solid lubricant and thus induces a decrease in the friction coefficient [7]; different abrasive particles, such as Al_2O_3, SiO_2, ZrO_2 that raise the friction coefficient [8]; Fe powder, to tune mechanical and tribological properties [4]. Similar Cu-graphite composites, but not containing abrasives, are used for electrical contacts against steel or Cu-based counterfaces (or Cu-coated steel parts) [9, 10]. In this case, great emphasis is placed on the graphite content and morphology, to optimize the electrical properties of the materials, being the frictional behaviour of the system not critically important, even if a low friction coefficient is beneficial for energy saving [11]. Cu-based metal-matrix composites are also produced with ceramic abrasive particles, such as SiC particles, and without graphite [12]. The aim is to obtain composites with high strength, because of the ceramic reinforcements, and high wear resistance [13].

In all cases, the friction and wear behaviour of the materials is determined by the characteristics of the friction layer that is formed during sliding. As originally proposed by Rigney et al. [14], during dry sliding metals undergo large plastic strains at the contact regions, because of adhesive interactions. These strains can induce the formation of wear debris. In Cu alloys, the phenomenon is aided further by the occurrence of shear instabilities [14]. As a consequence, alloy transfer onto the steel counterface may occur, followed by mixing with debris from the steel wear, thus forming a tribological layer at the interface between the mating surfaces. This interface layer is often called “tribo-layer” or Mechanically Mixed Layer (MML) [12, 15, 16]. Debris are often oxidized, because of the interaction with the surrounding atmosphere and the tribo-layer is thus formed by the agglomeration and compaction of oxides [12, 17-20]. The characteristics of the tribo-layer determine the friction and wear behaviour of the tribological system. In general, mild wear is associated with the formation of oxide-rich tribo-layers [12, 18-21]. Peng et al. [4] investigated the role of Cu/Fe ratio on the sliding behaviour and tribo-layer formation in Cu-based composites, containing also graphite and different abrasives, dry sliding against a forged steel. The Authors carried out sliding tests at a contact pressure of 1.1 MPa. A decrease in friction and wear with the decrease of the Cu/Fe ratio was highlighted and attributed to Fe that accelerates the formation of the tribo-layer and makes more difficult its disruption. The tribo-layer was found to be constituted by the compaction and sintering of oxides, mainly Fe-oxides (a mixture of Fe_3O_4, Fe_2O_3 and FeO), with a minor presence of cupric oxides (Cu_2O and CuO) that are comparatively less stable. Xiong et al. [8] investigated the dry sliding behaviour of a Cu-based PM composite containing Fe and SiO_2 powders. A structural steel was used as a counterface. The Authors found an increase in friction coefficient with Fe content and they observed the formation of a friction surface resulting from the compaction of oxides. The effect of SiO_2 particles on friction and wear turned out to be rather complex and depending on the sliding velocity. Clear evidence of formation of a friction layer of compacted oxide particles was also reported by Xiao et al [8], investigating the dry sliding behaviour of a Cu-base composite for brake pads. Zhan and Zhan [12], investigated the dry sliding behaviour of a Cu-base composite reinforced with 10 vol.-% of SiC particles, using a bearing steel as a

counterface. The worn surfaces exhibit a friction layer containing debris from both mating materials, including Cu- and Fe-oxides. Mechanical mixing was clearly accompanied by oxidation of the particles entrapped in between the contacting surfaces. The Authors highlighted the important role of the abrasive SiC particles, whose sharp edges were able to cut the steel counterface and produce Fe particles that were transferred onto the counterface and also oxidized by the environmental oxygen, depending on the surface temperature. Grandin and Wiklund [11] investigated the dry sliding behaviour of a Cu-graphite PM composite containing 26 vol.-% of copper and no abrasives. Sliding electrical contact was simulated using a spring steel as a counterface. Observations of the worn out surfaces revealed the presence of the tribo-layers with large strain localizations on both mating materials. However, the absence of abrasives in the Cu-base composite did not produce Fe debris, not even oxidized, and the layers were found to be made of metallic Cu and Cu_2O only.

It is clear that the tribological performance of the Cu-based composites sliding against steel is also dependent from the characteristics of the counterface steel, which plays an important role in the whole wear process. Hardness, for example, is important in the formation process of oxide-rich tribo-layers, resulting in a mild wear regime. The steel chemical composition might be also important to determine the relevant response to an oxidative reaction [2, 22-25]. However, this aspect is not widely investigated in the literature, since in most investigations just one steel counterface is used for the sliding tests and no compative tests are carried out. In the present investigation, the dry sliding behaviour of commercial Cu-based graphitic composite for brake applications sliding against three different steels with a martensitic microstructure is investigated. The tests were carried out using a pin-on-disc apparatus under constant sliding speed. Different contact pressures and sliding speeds were considered, to understand their role in the dry sliding behaviour of the materials under study, by means of a careful characterization of the friction layers that form on pins and discs during sliding.

2 Experimental procedures

2.1 Materials

The copper-based composite from which the pins for the sliding tests were extracted, is a commercial pad designed for high-speed train brakes. Figure 1 shows its microstructure as imaged using back-scattered electrons (BSEs) in a scanning electron microscope. The main constituents were identified, as indicated in the figure, by energy dispersive X-ray spectroscopy analyses. The main constituents are: graphite, Fe and Calcium fluoride (CaF_2) particles; abrasives, like ZrO_2, Al_2O_3 and SiO_2; the Cu-Sn matrix. Image analysis, using the ImageJ free software, provided a semiquantitative estimation of the content of the above constituents (in vol.%): graphite 15%, Cu-Sn matrix: 35%, Fe particles: 6%, CaF_2: 10%; SiO_2: 10%; Al_2O_3: 5%; ZrO_2: 5%.

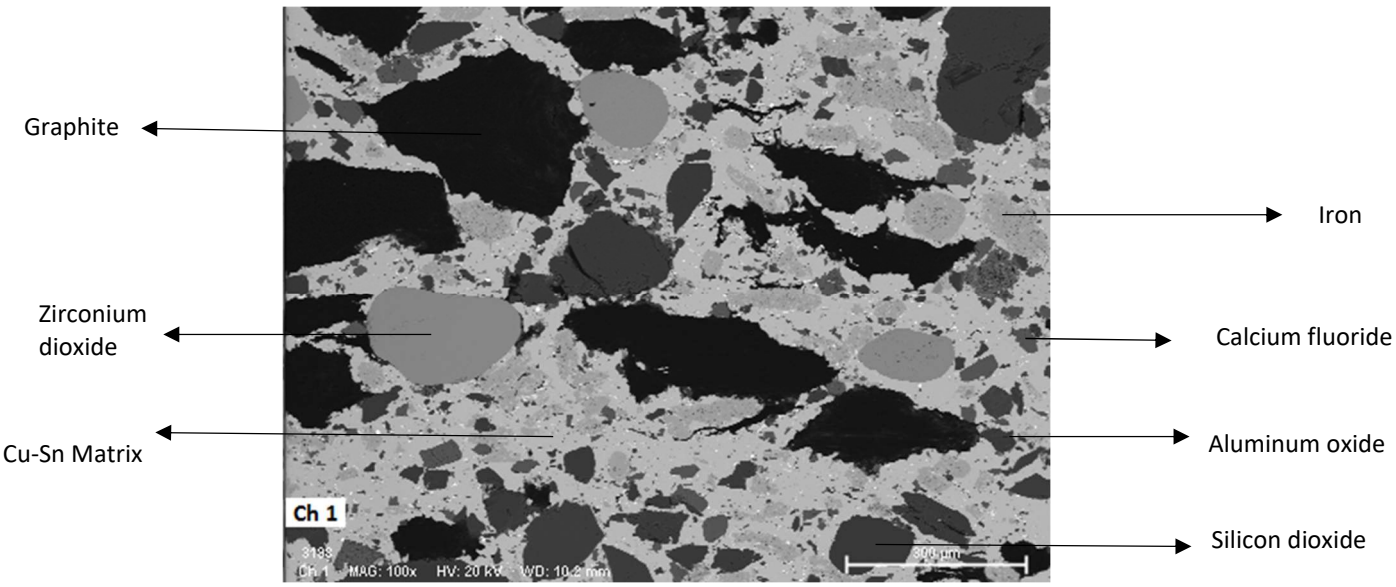

Fig. 1 Backscattered electron image of copper-based composite with the indication of the main ingredients.

Three commercial steels were used for the counterface discs. They are indicated with A, B and C, and their nominal chemical compositions are listed in Table 1. Steel A is a low-C martensitic stainless steel with high Cr-content, steel B is a low-alloyed steel, and steel C is a conventional martensitic stainless steel. Steel A is widely employed as counterface rotor for Cu-based sintered friction materials. Steel B and C were selected on the basis of their mechanical and microstructural features, as possible substitutes of steel A. All the steels were heat-treated, to obtain a martensitic microstructure, and then just stress-relieved, to retain the highest hardness levels and provide the best tribological behaviour. The hardness was measured using a Vickers indenter and a load of 30 kg (Table 1).

Table 1 Nominal composition, physical properties and Vickers hardness of the three steels under investigation (the thermal conductivities and the specific heats were taken from references [26-28]).

Steel	European standard	Nominal chemical composition, wt.%								Thermal Conductivity [W/mK]	Specific Heat [J/gK]	Hardness HV30
		C	Mn	Si	Cr	Ni	Mo	P	S			
A	X4CrNiMo 16-5-1	0.06			16	4	1			19	0.48	408
B	42CrMo4	0.42	0.8	0.2	1		0.2	0.02	0.02	45	0.47	334
C	X46Cr13	0.45	0.8	0.8	13	-	-	0.03	0.03	30	0.46	342

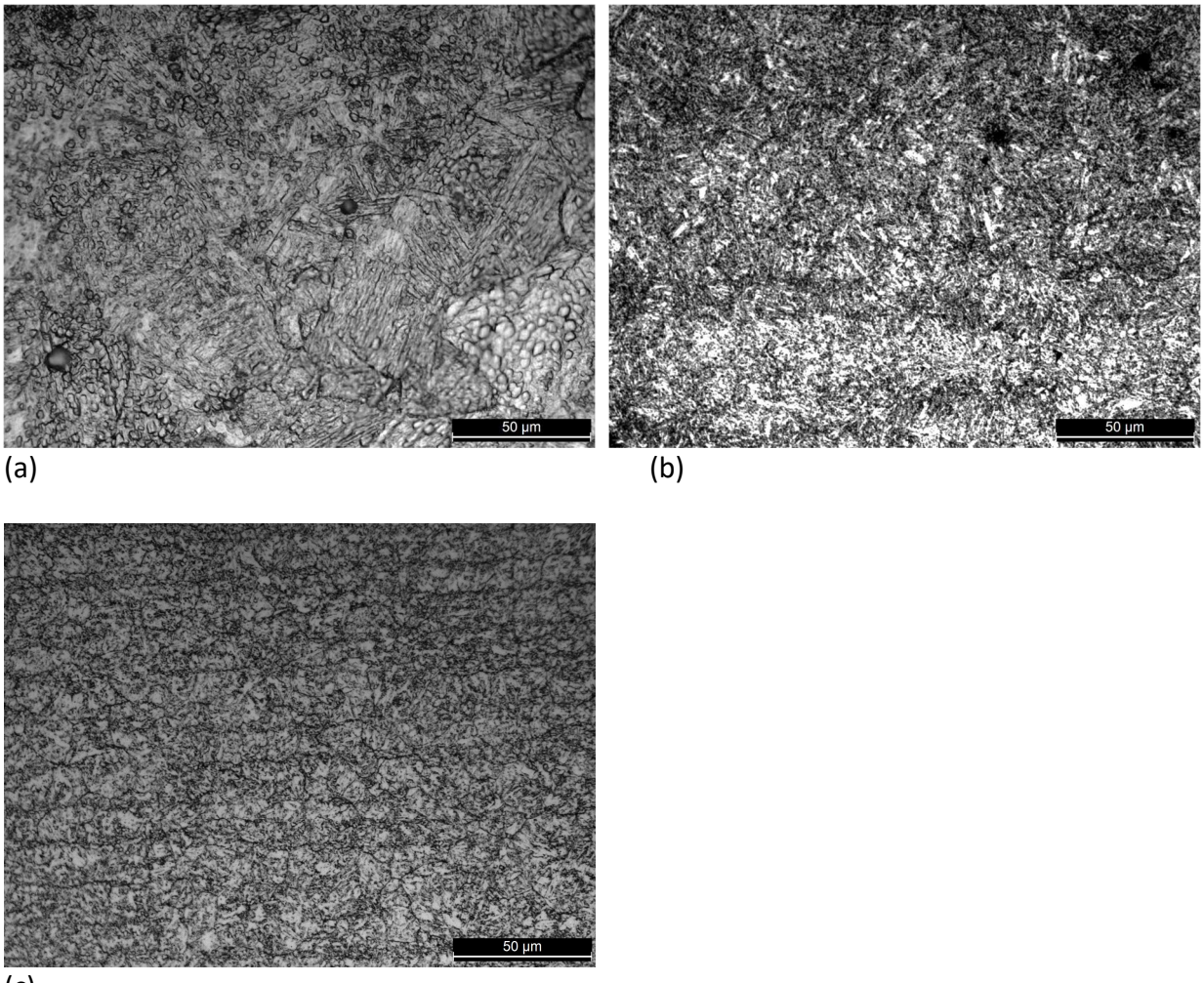

(a) (b)

(c)

Fig. 2 Microstructure of the steels under study. (a) steel A; (b) steel B; (c) steel C.

2.2 Pin-on-disc testing

Dry sliding tests were carried out at room temperature (22°C) using a Ducom pin-on-disc (PoD) testing rig. The discs had a diameter of 140 mm and a height of 15 mm. The pins were extracted from a commercial pad and had a diameter of 10 mm and a height of 12 mm. The tests were carried out at two nominal contact pressures (0.5 and 1 MPa) and two sliding speeds (1.57 and 7 m/s). The test duration was 1 h for all test conditions. During each test the coefficient of friction (COF) was continuously recorded. The disc surface temperature at 1 mm from the wear track was also recorded using a thermal camera. The surface of the disc was coated with high emissivity black paint in order to eliminate the reflection of infrared radiation from the shiny surface of steel [29].

The pin wear was measured by checking its weight before and after each test, using an analytical balance with a precision of 10^{-4} g. Wear volumes losses, V, were evaluated using a density of the copper-based material of 4.2 g/cm^3. From V and considering the sliding distance, d, and the applied load, F, the specific wear coefficient, K_a, was determined using the following equation:

$$K_a = V/F \cdot d \qquad 1.$$

The disc wear volume, V, was evaluated by means of a transverse profile obtained perpendicularly to the wear track [2] with a stylus profilometer.

2.3 Characterization of the worn surfaces

The surface morphology and composition of the worn pins and counterface discs were examined using an optical microscope and a scanning electron microscope (SEM) equipped with an energy dispersive X-ray spectroscopy (EDXS) system. To investigate the microstructure of the pins and discs close to the wear traces, metallographically prepared cross sections were also examined in the SEM. Microhardness measurements were performed on the disc cross-sections in the bulk as well as close to the worn surface, using a Vickers micro-indenter and a load of 25 grams.

3 Results

3.1 Friction and wear behaviour

Figure 3 shows the coefficient of friction (a) and disc temperature evolution with time (b), for the composite sliding against steel A at 0.5 MPa and 1.57 m/s. After a short run-in stage, the COF reaches a steady-state value (approximately 0.42). At the same time, the disc temperature increases from room temperature to a final value of approximately 100°C, taking a much longer time to reach equilibrium because of the thermal inertia of the disc. In Figures 4 and 5, all the recorded values of mean friction coefficients and disc surface temperatures at the end of each tests are summarized. It can be seen that the friction coefficients slightly decrease with the applied pressure and sliding velocity, with the only exception of steel C that shows an increase in the friction coefficient as sliding velocity is increased from 1.57 to 7 m/s. The surface temperature increases with the sliding velocity and contact pressure, despite of the decrease in the friction coefficient.

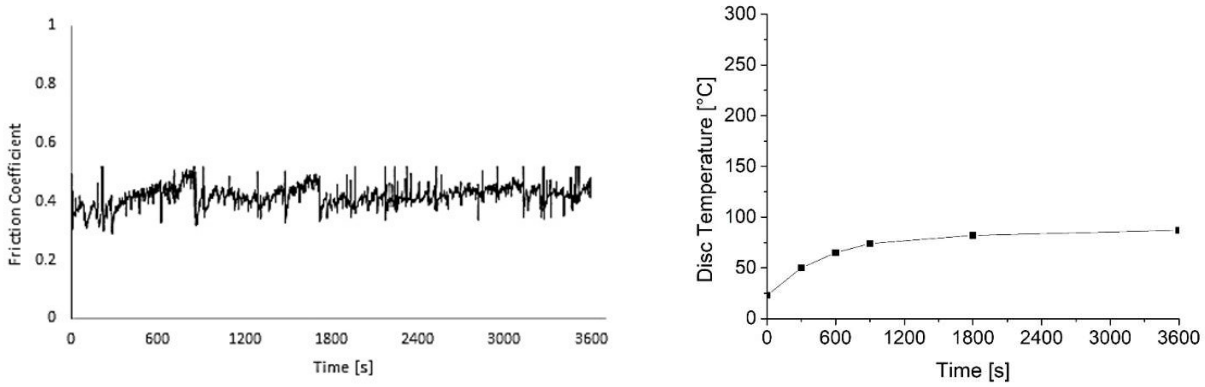

(a) (b)

Fig. 3 Evolution of the coefficient of friction (a) and surface temperature (b) for steel A tested at 0.5 MPa and 1.57 m/s.

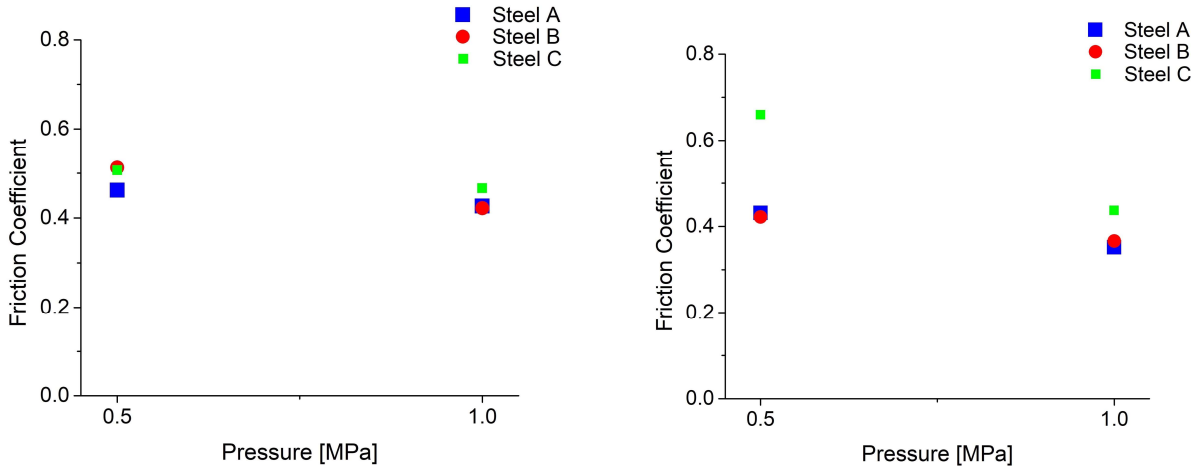

(a) (b)

Fig. 4 Mean coefficient of friction for (a) 1.57 m/s, and (b) 7 m/s.

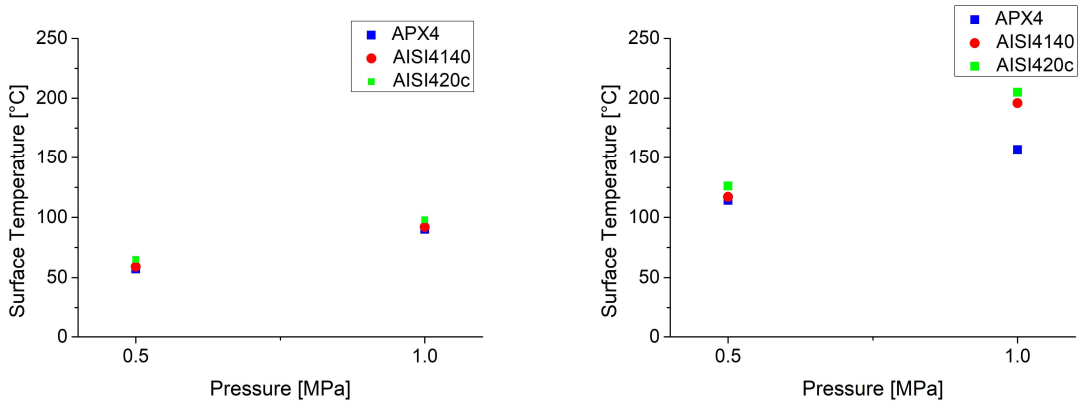

(a) (b)

Fig. 5 Surface temperature at the end of the tests 2 at (a) 1.57 m/s, and (b) 7 m/s.

The wear coefficients for the pins are plotted as a function of the contact pressure and for the two sliding speeds in Figure 6 (a) and b)). For steel A tested at 1.57 m/s only, wear is clearly severe, being K_a above 10^{-13} m^2/N. In all other cases, K_a is well below 10^{-13} m^2/N, i.e., in the mild wear regime [2, 24]. It can be also noted the K_a-values decrease as sliding speed is increased, whereas they are almost unaffected by contact pressure.

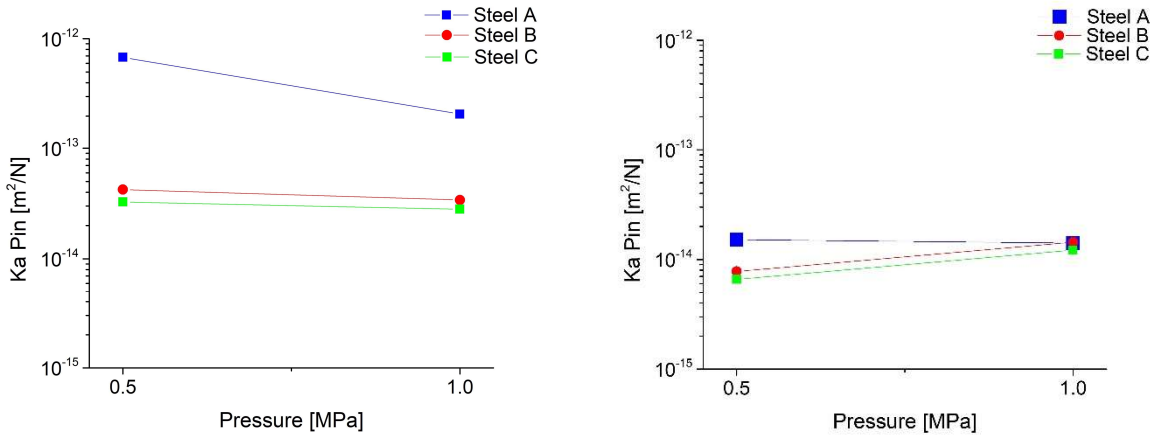

Fig. 6 K_a-values for pins at (a) 1.57 m/s, and (b) 7 m/s.

Figure 7 shows the surface profiles across the disc wear tracks in case of steel A after sliding at 0.5 MPa, and at 1.57 m/s (a) and 7 m/s (b). It is apparent that in the first case wear was quite intense, whereas in the second case it was quite limited. The obtained K_a-values for the discs are plotted in Figure 8, exhibiting trends very similar to those displayed by the pins (compare with Figure 6).

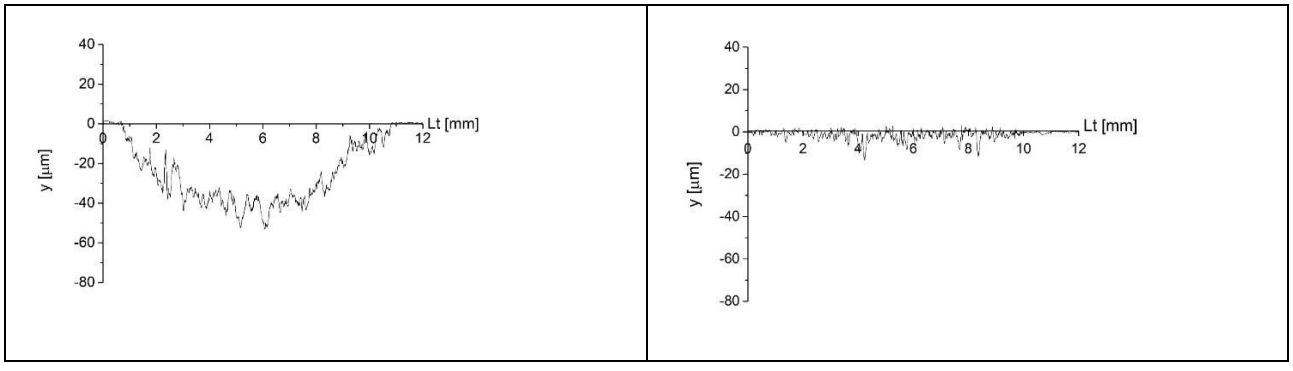

Fig. 7 Surface profiles across the wear traces for steel A tested at 0.5 MPa and at (a) 1.57 m/s, and (b) 7 m/s.

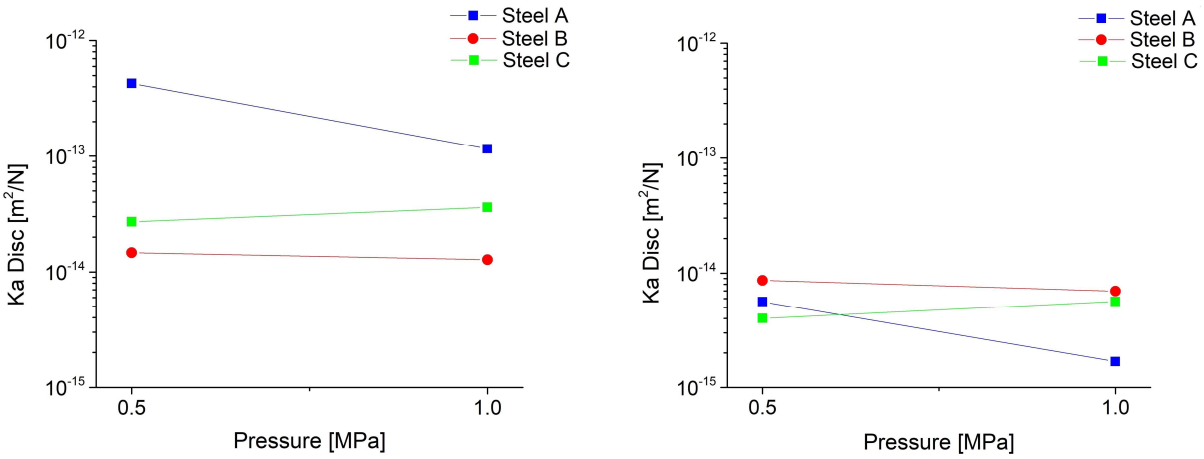

Fig. 8 K_a-values for the steel discs at (a) 1.57 m/s, and (b) 7 m/s.

3.2 Analysis of the pin worn surfaces

Figure 9 shows the pin worn surface after sliding against steel A at 1 MPa and 7 m/s. From EDXS analysis, it was possible to identify the main constituents of the friction layer, as indicated with arrows in Figure 9 (a) (alumina, graphite, calcium fluoride, silica, zirconia). Selected EDXS maps are also shown and they will help us in obtaining further information on the characteristics of the friction layer that formed on the pin worn surface. First of all, we can see that small areas looking white in Figure 9 (a) are made by the Cu-Sn alloy (the comparison with the oxygen map shows that almost no oxygen is present in these regions). Then we observe that the friction layer on the pin surface is mainly made by large grey areas that cover a large part of the worn surface. The EDXS maps reported in Figure 9 (b) show that such areas contain Fe, Cu, Ni, Cr and O. The comparison with literature observations show that such grey areas are typically made by the compaction of Fe-oxides [20, 22, 23, 30]. We see that such grey areas contain Fe, Ni and Cr and therefore wear fragments originating from the steel counterface (steel A; as shown in Table 1, it contains Cr and Ni). The Ni map shows that steel debris from the counterface are quite uniform in the friction layer, even if the Cr map shows that loose debris from the steel counterface are also present on the worn surface. The Fe, Cu and O-maps show that Fe/Cu-oxides may be actually present in the grey areas. In order to clarify this point we tried to obtain XRD-spectra on the worn surfaces using a Cr low-angle beam, but the signals were too weak to allow a correct identification of the present phases. We mainly detected the presence of haematite and magnetite, but the presence of Cu-oxides, often reported in the literature [4, 5], cannot be excluded. It can be also noted that graphite areas emerging at the surface are not covered by the oxides. This was already observed in different systems and it is due to the low surface energy of graphite and the consequent low adhesion versus the oxides [31].

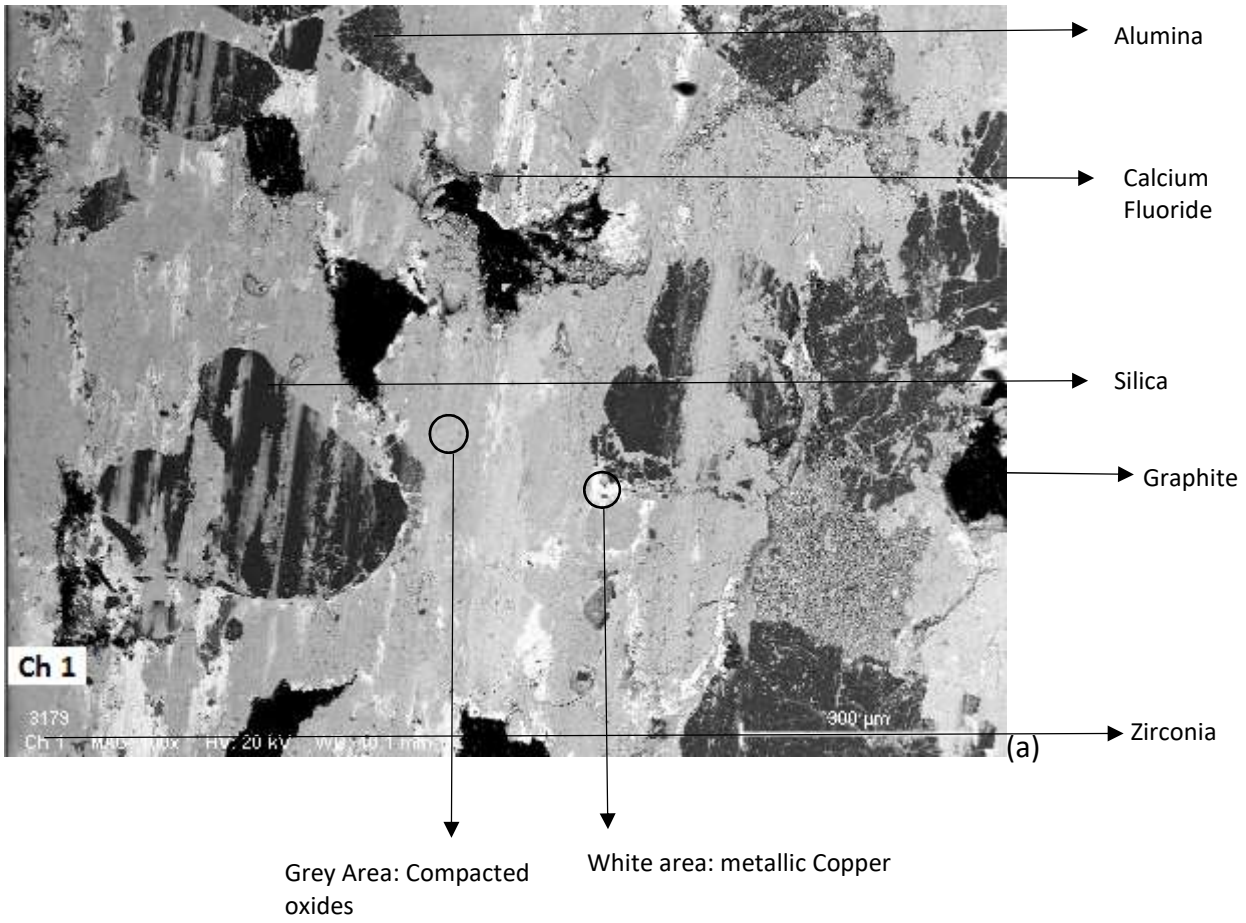

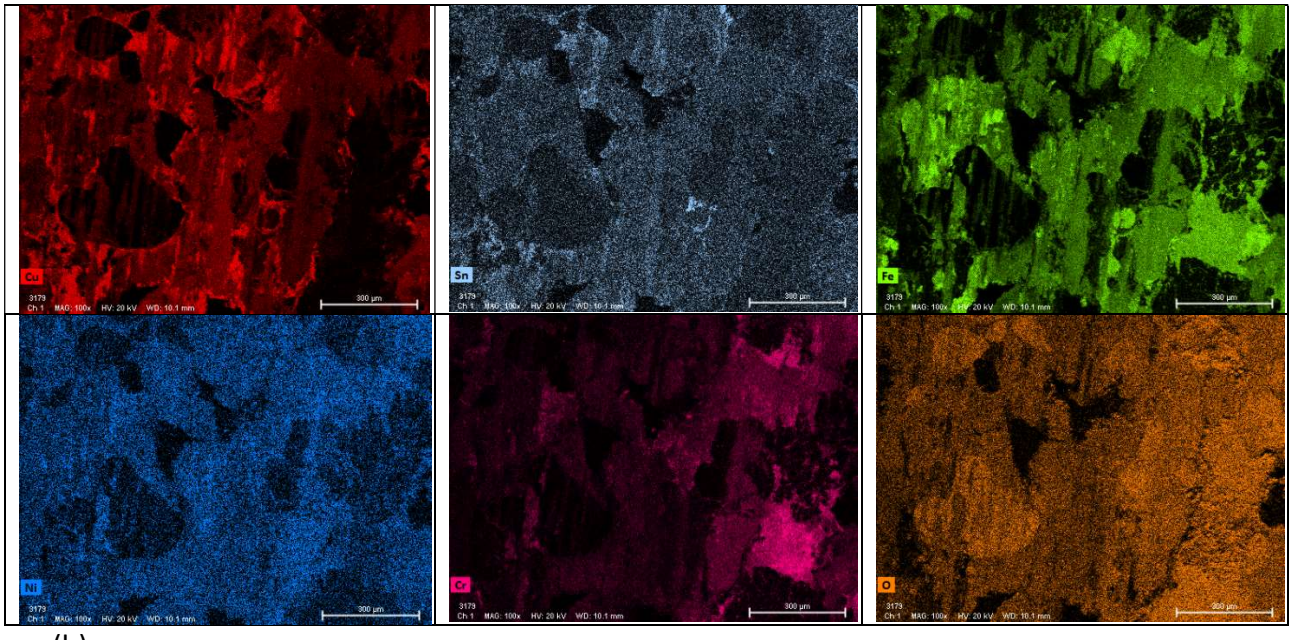

(b)

Fig. 9 (a) SEM micrograph of the copper-based composite pin after sliding against steel A at 1 MPa and 7 m/s with indication of the main ingredients; (b) EDXS maps of the main elements.

Similar observations were obtained for the other testing conditions, and also for the other steels. As an example, Figure 10 shows the worn surfaces of the pins tested at 0.5 MPa and 7 m/s against steel B (a) and steel C (b). It can be seen that some ingredients emerge at the surface and the worn surface is largely covered by a grey friction layer, with the exception of the black graphitic regions.

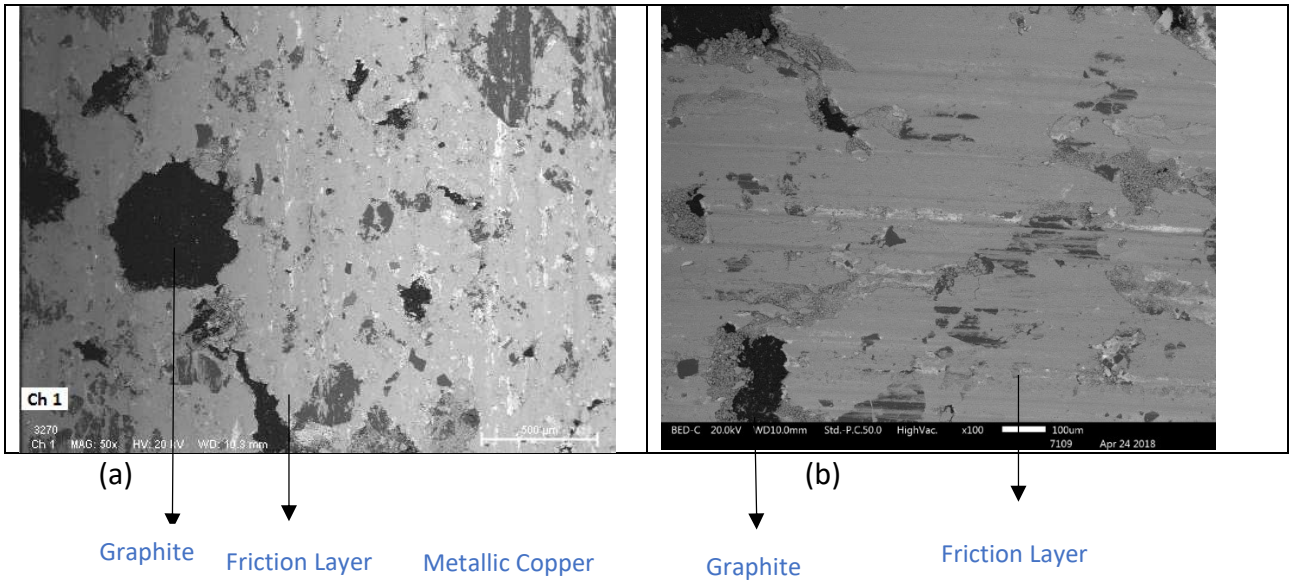

Fig. 10 SEM micrographs of the copper-based composite pin after sliding against steel B (a) and steel C (b) at 0.5 MPa and 7 m/s.

In order to get further information on the total amount of Fe- and Cu-oxides present in the friction layer on the composite surface, we carried out a full frame EDXS analysis of the elements. We then calculated the ratio: (Fe + Cu)/O, and the obtained values are listed in Table 2. To a first approximation, we can assume that as this ratio decreases, the amount of oxides in the friction layer (in particular Fe-oxides) increases. On the other hand, as the above ratio is increases, the amount of metallic elements (in particular Cu) increases too. This ratio appears quite high for steel A tested at 1.57 m/s (it is in excess of 10), whereas it appears lower for all the other cases (in the range 3.6 – 8). It is quite low, in the case of the tests at 7 m/s, in particular for steel C.

Table 2 (Fe + Cu)/O ratios obtained from the EDXS analyses of the pin friction layers.

Testing condition (MPa - m/s)	Steel A	Steel B	Steel C
0.5 – 1.57	13.5	7.9	5
1 – 1.57	10.3	8	5.9
0.5 – 7	7.45	5	3.6
1 - 7	5	5.28	4.35

Additional information on the characteristics of the friction layer (arrowed in Fig. 11) on the pin surfaces was achieved by observing the cross section of the worn samples, close to the worn surfaces. In Figure 11 (a), the cross section of the friction layer in case of steel A tested at 0.5 MPa

and 1.57 m/s is shown. The friction layer appears poorly adherent to the substrate and largely cracked, showing that wear was by adhesion/delamination. The EDXS analysis of the friction layer revealed the presence of a large presence of Cu (40.6 wt.%) and Fe (32.8 wt.%) concentrations. The ratio (Fe + Cu)/O is quite high (13.57), in agreement with the data shown in Table 3. This shows that a very few oxides were present in the friction layer. The situation changes by increasing the sliding velocity to 7 m/s, Figure 11 (b). Here the friction layer is clearly mainly made by the compaction of oxides. From the EDXS analysis, it turns out that the ratio (Fe + Cu)/O is 6.9. As a further example, in Figure 11 (c) the friction layer for steel B, tested at 1 MPa and 7 m/s. Here we observe the presence of compacted oxides sustained by a Cu region that underwent a large plastic deformation by shearing. The friction layer made by compacted oxides is clearly representative of the cross section of the grey areas shown in Figures 9 and 10.

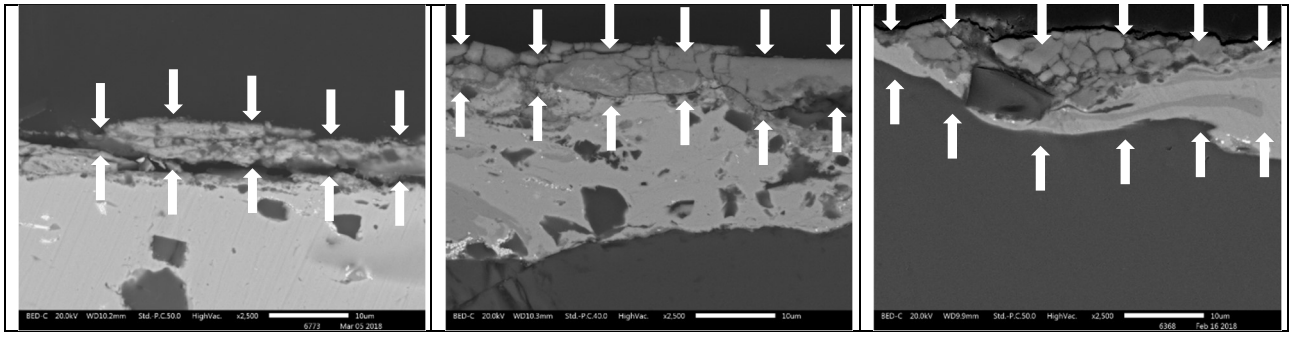

(a) (b) (c)

Fig. 11 Cross sectional microstructures showing the friction layers. (a) Steel A tested at 0.5 MPa and 1.57 m/s; (b) steel A tested at 0.5 MPa and 7 m/s; (c) steel B tested at 1 MPa and 7 m/s.

3.3 Analysis of the disc worn surfaces

Figure 12 (a) shows the worn surface of the disc made with steel A, at the end of the test at 0.5 MPa and 1.57 m/s. The presence of large plastic deformations in the direction of sliding can be clearly appreciated, which is representative of wear by adhesion/delamination [2, 22]. The full frame EDXS analysis highlighted the presence of Cr and Ni with amounts very similar to the steel composition (13.34 wt.% Cr and 4wt.%Ni), and the presence of some Cu due to the transfer from the pin counterface (9.23 wt.% Cu). The oxygen content is quite low (3.72 wt.%) and the ratio (Fe + Cu)/O is 20, showing that wear was mainly metallic in nature, in agreement with the observations of the corresponding pin surface. Figure 12 (b) shows the worn surface of the disc made with steel A, at the end of the test at 1 MPa and 7 m/s. In this case the worn surface is characterized by the presence of white and grey areas. The EDXS analysis on the white areas evidenced that they are very similar to the worn surface of the disc tested at 0.5 MPa and 1.57 m/s. On the average, the Cu content is 7.44 wt.% and the oxygen content is 5.7 wt.%. On the contrary, the grey areas contain 32 wt.% Cu and 13.2 wt.% oxygen (on the average). This shows that the grey areas are made by the compaction of Fe- and Cu-oxides [30]. This is also in agreement with the observations of the corresponding pin surfaces. In case of steels B and C, the worn surface of the samples tested at 1.57 m/s were always characterized by the presence of white and some grey areas, whereas the surfaces of the samples tested at 7 m/s were covered by large grey areas. As an example, Figures 12 (c) and (d) show the

worn surfaces of the discs made with steel C. The presence of a large oxide layer that spread on the worn surface of the disc tested at 7 m/s can be clearly appreciated.

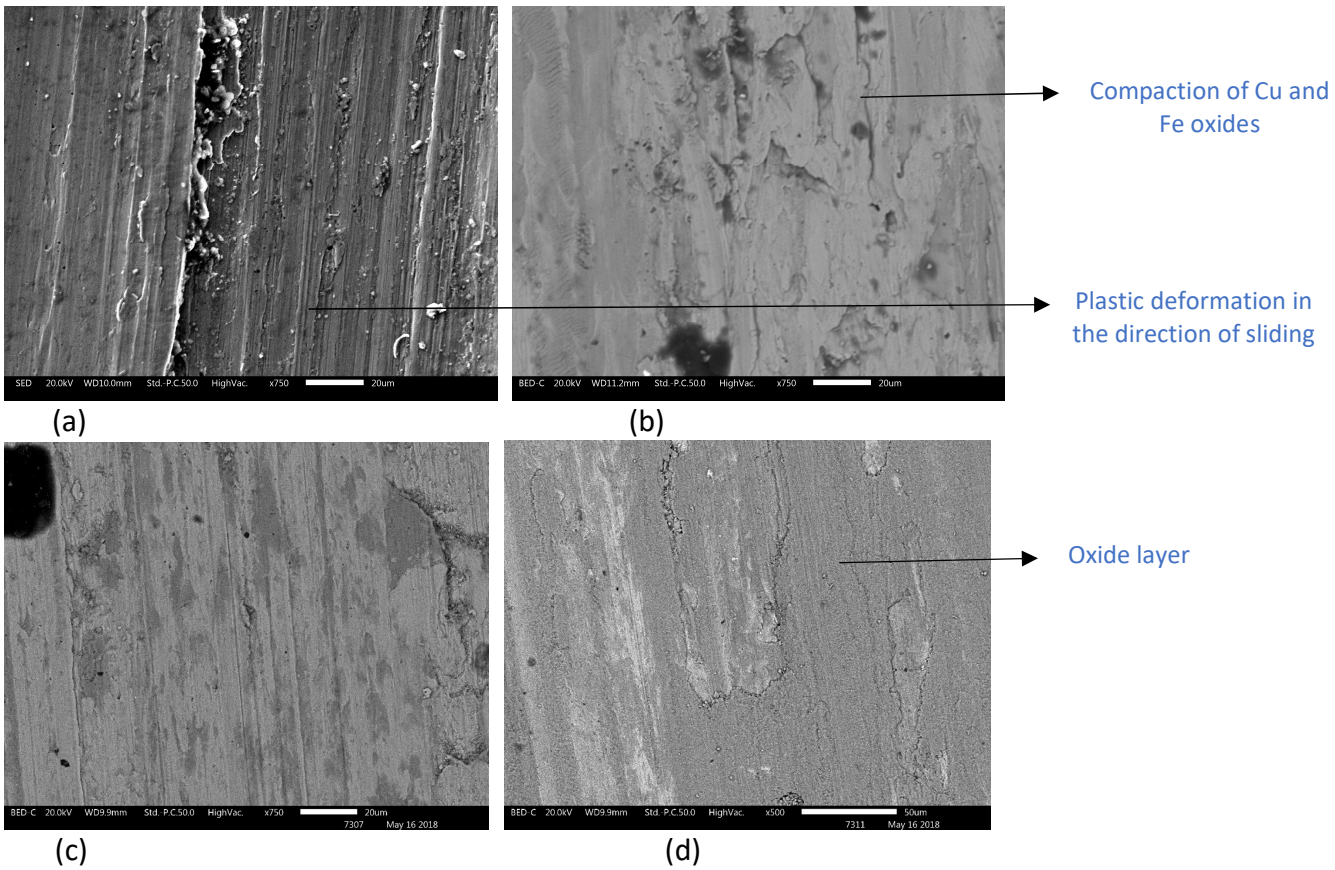

Fig. 12 SEM micrographs showing the top view of the wear trace of steel A after sliding at 0.5 MPa and 1.57 m/s (a) and at 1 MPa and 7 m/s (b), and of steel C after sliding at 0.5 MPa and 1.57 m/s (c) and at 1 MPa and 7 m/s (d).

To complete the picture, we carried out some microhardness measurements on the cross sections of the worn discs, with reference to the tests carried out at the lowest pressure and lowest velocity, that produced the lowest surface temperature rise during sliding, and the tests carried out at the highest pressure and highest velocity, that produced the biggest surface temperature rise during sliding. The measurements were obtained close to the worn surface and in the bulk (at a distance of approximately 200 μm from the worn surface). The obtained results are listed in Table 3. In case of steels B and C, an increase in microhardness was recorded close to the worn surface with respect to the bulk, showing that steel strain hardening was attained during sliding. On the contrary, in case of steel A, almost no change in the microhardness was detected, probably because of the high initial hardness of the steel and the corresponding negligible ability to undergo additional strain hardening [32].

Table 3 Microhardness values of the steel discs taken in the bulk and close to the worn traces.

Steel	Testing Conditions	Bulk Microhardness HV0.025	Microhardness Under the wear track HV0.025
A	0.5 MPa – 1.57 m/s	478 ± 6	476 ± 4
	1 MPa - 7 m/s	484 ± 4	479 ±7
B	0.5 MPa – 1.57 m/s	361 ± 3	440 ± 20
	1 MPa – 7 m/s	360 ± 3	385 ± 9
C	0.5 MPa – 1.57 m/s	393 ± 6	483 ± 23
	1 MPa – 7 m/s	390 ± 7	530 ± 29

4 Discussion

The specific wear rates, K_a, of the copper based composite under study are plotted in Figure 13 as a function of the (Fe + Cu)/O ratio relevant to the pin friction layer. It turns out that the K_a-values decrease as the (Fe + Cu)/O ratio decreases, showing that an increase in the fraction of oxides in the friction layer is beneficial to the wear resistance of the material, in agreement with the already reported observation that an oxide-rich and well compacted friction layer protects the underlying material from severe adhesion/delamination wear. As shown in the previous section, the wear mechanisms on the copper base composite pins and the corresponding steel discs are quite similar. This also explains the proportionality between the pin K_a-values and the disc K_a-values shown in Figure 14.

From the data in Figure 13 emerges that wear is always 'very mild', i.e., below 2 10^{-14} m^2/N, in the tests at 7 m/s, irrespective of the steel and contact pressure. As concerns the tests at 1.57 m/s, wear is mild too, i.e., below 4 10^{-15} m^2/N, for steels B and C, whereas, it is severe, i.e., K_a is above 10^{-13} m^2/N, for steel A.

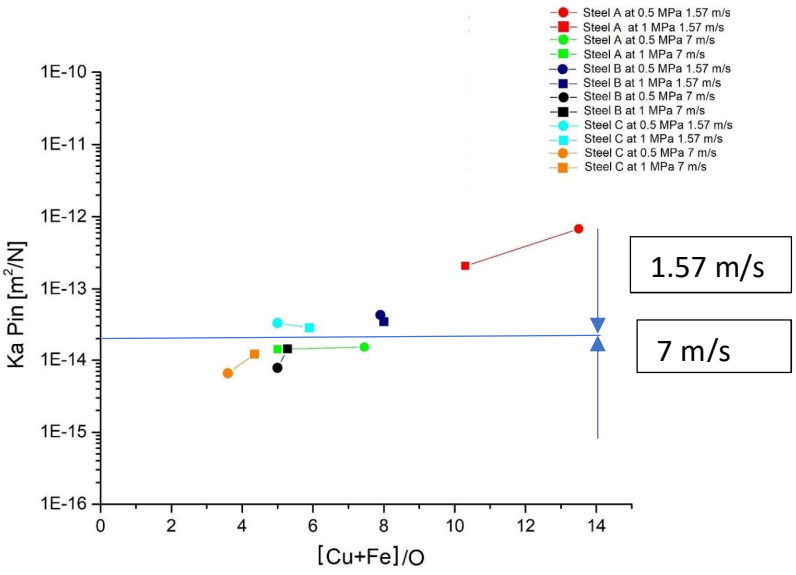

Fig. 13 Specific wear coefficient of pin vs. the (Fe + Cu)/O ratio.

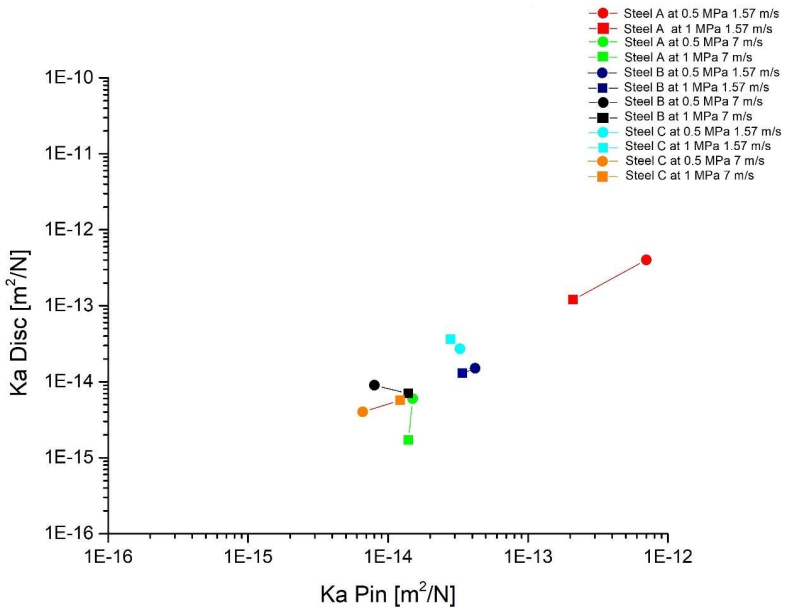

Fig. 14 Pin specific wear coefficient vs. disc specific wear coefficient.

In order to explain these results, we have to consider in detail the acting wear mechanisms. In this regard, it is important to evaluate the flash temperature reached during sliding. The flash temperature, T_f, is the temperature reached for a very short time at the contacting asperities during sliding, and due to the dissipation of the frictional energy. Using the approach proposed by Ashby et al. [25, 33], it can be supposed that the frictional heat is injected only across the real contact area, A_r, to reach the sink average surface temperature at specific distances that are called the 'equivalent diffusion distances' for the flash temperature, l_1 and l_2. Ashby et al. [25, 33] proposed some simplified relationships for A_r, l_1, l_2 and the extension of the contact junctions assuming a plastic contact. Using these relationships and the corresponding heat model, the following equation for a simplified evaluation of T_f can be obtained [2]:

$$T_f - T_s = 8.8\ 10^4 \frac{\mu}{\sqrt{1+12\ \mu^2}} \frac{v}{k_1+k_2} \qquad 2.$$

where T_s is the surface average temperature, μ is the average friction coefficient recorded during sliding, v is the sliding velocity and k_1 and k_2 are the thermal conductivities of the materials in contact. The μ-values were taken from Figure 4. The T_s-values were obtained from the experimental values of the surface temperature reported in Figure 5. In fact, previous investigations based on FE modelling, showed that the surface temperature measured in this way is close to the mean surface temperature in the wear track that, in turn, is also very close the average contact temperature [29, 34]. Within the limits of the approach, we therefore identified the surface temperatures in Figure 5 with the T_s-values to be used in equation 2. The thermal conductivities of the three steels under study were taken from specific datasheets [26-28]. They were assumed to be 19, 45, and 30 W/mK for steel A, B and C, respectively. Since we did not have the k-value for the copper based composite, we indirectly estimated it using specific temperature measurements at 1.57 m/s against steel A by

placing a thermocouple in the pin at a distance of 6 mm from the sliding surface, and the fitting temperature model proposed in [34]. The obtained result was 26 W/mK, in a good agreement with literature values for similar materials [1]. The results of the flash temperatures calculations, relevant conditions and main wear mechanisms are summarised in Table 3.

Table 5 Calculated flash temperatures and proposed wear mechanism in different testing conditions.

Steel	Testing Conditions	Flash Temperature [°C]	Wear mechanism
A	0.5 MPa – 1.57 m/s	860	Adhesion/delamination (severe wear)
	1 MPa – 1.57 m/s	882	Adhesion/delamination (sever wear)
	0.5 MPa – 7 m/s	> 1500	Intense oxidation (very mild wear)
	1 MPa – 7 m/s	>1500	Intense oxidation (very mild wear)
B	0.5 MPa – 1.57 m/s	588	Low-sliding speed oxidation (mild wear)
	1 MPa – 1.57 m/s	575	Low-sliding speed oxidation (mild wear)
	0.5 MPa – 7 m/s	> 1500	Intense oxidation (very mild wear)
	1 MPa – 7 m/s	>1500	Intense oxidation (very mild wear)
C	0.5 MPa – 1.57 m/s	690	Low-sliding speed oxidation (mild wear)
	1 MPa- 1.57 m/s	704	Low-sliding speed oxidation (mild wear)
	0.5 MPa – 7 m/s	>1500	Intense oxidation (very mild wear)
	1 MPa – 7 m/s	>1500	Intense oxidation (very mild wear)

Let us consider first the 'very mild' wear, displayed by the discs and the pins tested at 7 m/s. Irrespective of the steel and the contact pressure, the calculated flash temperature is always very high, above 1500°C, in agreement with data reported in [25,33]. This means that the asperity oxidation of the steel contact surfaces was very easy and fast and this justifies an intense oxidation. The same is not true for the pin asperities, since it is known that copper oxides are rather unstable at these temperatures. As a consequence, iron oxides easily formed and spread over the worn out surfaces, both of pin and disc, as shown by Figures 9, 12 (b) and 12 (c). It is also suggested that the very high flash temperature induced a substantial softening or even melting of the oxides during sliding, which greatly favoured compaction and spreading on the worn surfaces. Because of the high flash temperature, any influence of the specific steel composition can be neglected, and wear is tribo-oxidative and mild in character, independently from steel composition and contact pressure.

Consider now the wear behaviour of pins and discs at 1.57 m/s. The calculated flash temperatures for the three steels are still quite high: around 580°C for steel B, 700°C for steel C and 870°C for steel A. In all cases the flash temperature appears sufficiently high to induce the oxidation of the asperities, and then mild tribo-oxidative wear. As a matter of fact, this occurred for steels B and C, but not for steel A. This behaviour can be explained considering that steel A is characterized by a very low oxidation tendency, because it contains a high amount of Cr and a very low amount of C (incidentally, the excellent corrosion resistance of steel A was also confirmed by the high difficulty encountered in the metallographic etching). As clearly explained by Vingsbo and Hogmark [22], the inherent high oxidation resistance of a steel renders very difficult the oxidation of the asperities and also of the entrapped wear fragments between the contacting surfaces of the pin and disc. Therefore, wear may occur mainly by adhesion/delamination.

The tribo-oxidative wear of steels B and C at 1.57 m/s is different from the tribo-oxidative wear of all the steels at 7 m/s. At 1.57 m/s , no nearly continuous oxide layer was observed on the worn surface, but rather discrete oxide islands on the worn surfaces. These observations are typical of the so-called 'tribo-oxidative wear at low-sliding speeds' [35]. It is believed that iron oxides were formed by direct asperity oxidation and also by oxidation of heavily deformed metallic fragments formed during the run-in stage, as proposed by Stott and co-workers [20]. The flash temperature was not sufficiently high to sustain the kinetics of extensive oxidation and plastic spreading of the soft oxides on the wear surface, as it occurred at 7 m/s. In any case, steel C is characterized by the lowest specific wear coefficient among the steels here considered, because of its ability to sustain the oxide-rich friction layer during sliding because of its high hardness and high strain-hardening ability. Indeed, with an increase of the subsurface hardness, the ability of the steel to maintain the surface oxide layer in its place also increases.

Finally, we consider the friction behaviour of the materials under study. In Fig. 15, the average steady-state values of the friction coefficient (taken from Fig. 4), are plotted as a function of the (Fe + Cu)/O ratio referring to the pin friction layer. It can be observed that friction coefficient increases as the (Fe + Cu)/O ratio decreases and two distinct trends are displayed at the two sliding velocities. The obtained results will be explained, in the following lines, within the frame of the adhesive theory of friction [2, 37, 38]. In fact, a decrease in the (Fe + Cu)/O ratio corresponds to an increase in the fraction of Fe-oxides in the pin friction layer and thus an increase in the work of adhesion between the pin and the steel disc counterface [36]. The value of the friction coefficient of 0.65 for steel C at 7 m/s and the relevant high coverage of the oxide-rich friction layer of the wear surface is typical of the Fe oxide-Fe oxide contact under dry sliding conditions [39]. On the contrary, the value of the friction coefficient of approximately 0.4 for steel A at 1.57 m/s and with an almost negligible fraction of oxides on the wear surface, is typical of the metallic steel-Cu alloys under dry sliding conditions [39]. In addition, the average friction coefficient decreases as the sliding speed is increased, since less time is allowed to the asperity contacts to form tough junctions, as commonly observed in other tribological systems [40].

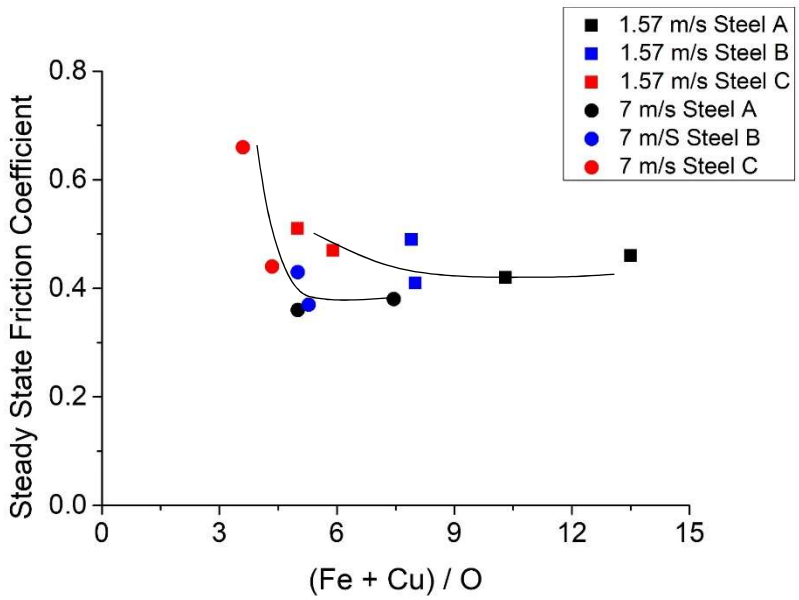

Fig. 15: Steady state friction coefficient as a function of the (Fe+Cu)/O ratio.

5 Conclusions

Pin-on-disc tests were conducted at room temperature to investigate the dry sliding behaviour of a commercial copper-based metal matrix composite pin (containing graphite and abrasive oxides) against three types of martensitic steel discs, having different chemical composition. The main results can be summarized as follows:

- When using steel A at 1.57 m/s and 0.5 MPa, the dominant wear mechanism of both the pin and the disc was by adhesion/delamination. Therefore, wear was metallic and severe. In fact, the high Cr- and low C-content of steel A made it highly resistant to oxidation, making very difficult the possibility to have tribo-oxidative wear.
- When using steel A at 1.57 m/s and at 1 MPa, and steels B and C at 1.57 m/s and at 0.5 and 1 MPa, both pin and discs underwent moderate tribo-oxidative wear. The pin and disc surfaces were covered and protected by islands of oxide-rich friction layers, mainly made of Fe-oxides from the disc wear. The sub-surface hardening in steels B and C enhanced their capability of properly sustain the oxide-rich friction layer.
- In all cases, pin and discs underwent very mild tribo-oxidative wear at 7 m/s. This can be ascribed to the very high contact flash temperatures achieved during sliding. These temperatures promoted an easy oxidation of the mating asperities independently from chemical composition of the steel discs.
- Since pins and discs exhibited similar wear mechanisms under the same sliding conditions (i.e., at the same contact pressure and sliding velocity), a direct relationship between the specific wear coefficient of the pin and the disc was obtained.
- The average friction coefficients were found to decrease as the (Fe + Cu)/O ratio, relevant to the pin friction layer, increases and as the sliding velocity increases. These results were explained in the frame of the adhesive theory of friction.
- The results obtained in this investigation show that a proper selection of the steel counterface is paramount to optimize the friction and wear behaviour of the copper based composite/steel tribological system. The results show that steel C, a conventional martensitic stainless steel, is characterized by the lowest pin and disc specific wear rates and the highest values of the friction coefficient, due to its ability to produce and sustain an oxide-rich friction layer.

Acknowledgments:
The Authors wish to thank Lorena Maines and Alberto Zanellini for wear testing and characterization support.

References

[1] Glaeser, W.A:. Materials for tribology, Tribology series 20, Elsevier (1992).

[2] Straffelini, G.: Friction and Wear, Methodologies for Design and Control, Springer International Publishing, Switzerland (2015).

[3] Mann, R., Magnier, V., Brunel J-F., Brunel F., Dufrenoy, P., Henrion, M.: Relation between mechanical behavior and microstructure of a sintered material for braking application, Wear 386-387, 1-16 (2017).

[4] Peng, T., Yan, Q., Li, G., Zhang, X.: The influence of Cu/Fe ratio on the tribological behavior of brake friction materials, Tribol. Lett. 66:18 (2018).

[5] Peng, T., Yan, Q., Li, G., Zhang, X., Wen, Z., Jin, X.: The braking behavior of Cu-based metallic brake pad for high-speed train under different initial braking speed, Tribol. Lett., 65:135 (2017).

[6] Xiao, Y., Zhang, Z., Yao, P., Fan, K., Zhou, H., Gong, T., Zhao, L., Deng, M.: Mechanical and tribological behaviors of copper metal matrix composites for brake pads used in high-speed trains, Tribol. Int. 119, 585-592 (2018).

[7] Su, L., Gao, F., Han, X., Fu, R., Zhang, E.: Tribological behavior of Copper-graphite powder third body on copper-based friction materials, Tribol. Lett. 60:30 (2015).

[8] Xiong, X., Chen, J., Yao, P., Li, S., Huang, B.: Friction and wear behaviors and mechanisms of Fe and SiO_2 in Cu-based P/M friction materials, Wear 262, 1182-1186 (2007).

[9] Yasar, I., Canakci, A., Arslan, F.: The effect of brush spring pressure on the wear behaviour of copper-graphite brushes with electrical current, Tribol. Int. 40, 1381-1386 (2007).

[10] Moustafa, S.F., El-Badry, S.A., Sanad, A.M., Kiebak, B.: Friction and wear of copper-graphite composited made with Cu-coated and uncoated powders, Wear 253, 699-710 (2002).

[11] Grandin, M., Wiklund, U.: Influence of mechanical and electrical load on copper/copper-graphite sliding electrical contact, Tribol. Int. 121, 1-9 (2018).

[12] Zhan, Y.Z., Zhang, G.: Mechanical mixing and wear-debris formation in the dry sliding wear of copper matrix composite, Tribol. Lett., Vol. 17, No. 3 (2004).

[13] Wilson, S., Alpas, A.T.: Wear mechanism maps for metal matrix composites, Wear 212, 41-49 (1997).

[14] Rigney, D.A., Chen, L.H., Naylor., M.G.S.: Wear processes in sliding systems, Wear 100, 195-219 (1984).

[15] Venkataraman, B., Sundararajan, G.: Correlation between the characteristics of the mechanically mixed layer and wear behaviour of aluminium, Al-7075 alloy and Al-MMCs, Wear 245, 22-38 (2000).

[16] Straffelini, G., Bonollo, F., Molinari, A., Tiziani. A.: Influence of matrix hardness on the dry sliding behaviour of 20 vol.% Al_2O_3-particulate-reinforced 6061 Al metal matrix composite, Wear 211, 192-197 (1997).

[17] Straffelini, G.: Experimental observations of subsurface damage and oxidative wear in Al-based metal-matrix composites, Wear 245, 216-222 (2000).

[18] Scardi, P., Leoni, M., Straffelini, G., De Giudici, G.: Microstructure of Cu-Be alloy triboxidative wear debris, Acta mater. 55, 2531-2538 (2007).

[19] Quinn, T.F.J., Sullivan, J.L., Rowson, D.M.: Origins and development of oxidational wear at low ambient temperatures, Wear 94, 175-191 (1984).

[20] Stott, F.H., The role of oxidation in the wear of alloys, Tribol. Int. 31, 61-71 (1998).

[21] Zhang, J., Alpas, A.T.: Transition between mild and severe wear in aluminium alloys, Acta mater. 45, 513-528 (1997).

[22] Vingsbo, O., Hogmark, S.: Wear of steels, in: Fundamentals of friction and wear of materials, D.A:, Rigney, ed., ASM, Materials Park, Ohio, USA, 41-52 (1980).
[23] Straffelini, G., Trabucco, D., Molinari, A.: Oxidative wear of heat-treated steels, Wear 250, 485-491 (2001).
[24] Straffelini, G., Trabucco, D., Molinari, A.: Sliding wear of austenitic and austenitic-ferritic stainless steels, Met. And Mat. Transactions 33A, 613-624 (2002).
[25] Lim, F.C., Ashby, M.F.: Wear mechanism maps, Acta metal. 35, 1-24 (1987).
[26] APX4 steel data sheet, Aubert%Duval (www.aubertduval.com).
[27] A.S.M., Properties and selection: Iron, steel and high performance alloys, Metals Handbook, 10th ed., vol. 1, ASM Materials Park, Ohio, USA (1992).
[28] CRC Handbook of Chemistry and Physics toth edn., CRC Press, Cleveland, Ohio, USA (1989-90).
[29] Straffelini, G., Verlinsky, S., Verma, P.C., Valota, G., Gialanella, S.,: Wear and contact temperature evolution in Pin-on-Disc tribotesting of low metallic friction material sliding against pearlitic cast iron, Tribol. Lett. 62:36 (2016).
[30] Riahi, A.R., Alpas, A.T.: Wear map for grey cast iron, Wear 255, 401-409 (2003).
[31] Lee, P.W., Filip, P.: Friction and wear of Cu-free and Sb-free environmental friendly automotive brake materials, Wear 302, 1404-1413 (2013).
[32] Li, W., Wang, Y., Yang, X.Z.: Frictional hardening and softening of steel 52100 during dry sliding, Tribol. Lett. Vol. 18, No.3 (2005).
[33] Ashby, M.F., Kong, H.S., Abulawi, J.: T-maps: User manual, Cambridge University Press, Cambridge (1991).
[34] Federici, M., Straffelini, G., Gialanella, S.: Pin-on-Disc testing of low metallic friction material sliding against HVOF coated cast iron: modelling of the contact temperature evolution, Tribol. Lett. 65:121 (2017).
[35] Stachowiak, G.W., Batchelor, A.W.: Engineering Tribology, Tribology Series 24, Amsterdam, Elsevier (1993).
[36] B. Bushan, Introduction to tribology, second edition, John Wiley & Sons, Ltd (2013).
[37] K. Miyoshi, Solid Lubrication, Fundamentals and Applications, Marcel Dekker, Inc., New York, USA (2001).
[38] Straffelini, G.: A simplified approach to the adhesive theory of friction, Wear 249, 79-85 (2001).
[39] Lim, S.C., Ashby, M.F., Brunton, J.H.: The effects of sliding conditions on the dry friction of metals, Acta metal. 37, 767-772 (1989).
[40] E. Rabinowicz, Friction and wear of materials, 2nd ed., Wiley (1995).